Original Article

Particle swarm optimization and spiral dynamic algorithm-based interval type-2 fuzzy logic control of triple-link inverted pendulum system: A comparative assessment

MF Masrom[1] ⬤, NMA Ghani[1] and MO Tokhi[2]

Abstract
This paper presents investigations into the development of an interval type-2 fuzzy logic control (IT2FLC) mechanism integrated with particle swarm optimization and spiral dynamic algorithm. The particle swarm optimization and spiral dynamic algorithm are used for enhanced performance of the IT2FLC by finding optimised values for input and output controller gains and parameter values of IT2FLC membership function as comparison purpose in order to identify better solution for the system. A new model of triple-link inverted pendulum on two-wheels system, developed within SimWise 4D software environment and integrated with Matlab/Simulink for control purpose. Several tests comprising system stabilization, disturbance rejection and convergence accuracy of the algorithms are carried out to demonstrate the robustness of the control approach. It is shown that the particle swarm optimization-based control mechanism performs better than the spiral dynamic algorithm-based control in terms of system stability, disturbance rejection and reduce noise. Moreover, the particle swarm optimization-based IT2FLC shows better performance in comparison to previous research. It is envisaged that this system and control algorithm can be very useful for the development of a mobile robot with extended functionality.

Keywords
Interval type-2 fuzzy logic control, spiral dynamic algorithm, particle swarm optimization

Introduction

Self-balancing inverted pendulum systems have attracted a lot of interest within the research community. Inverted pendulum is an under actuated system and able to achieve stability after facing a disturbance by obstacles or while moving on a sloped path. The main control challenges are to achieve fast settling time and low state steady error while in the upright position. Inverted pendulum systems vary from single link, double, and triple links.

Recent research in triple-link pendulum has considered pendulum on cart systems. For example, Sharma and Sahu[1] used Lagrange equation to model a triple-link inverted pendulum on cart system and linearized it to design a linear quadratic regulator (LQR) using single output. The system described in Wei et al.[2] used triple-link inverted pendulum on cart system and adaptive neural-fuzzy inference system (ANFIS) for its control. The proposed of this new system of triple links inverted pendulum on two-wheeled is due to the limitation of modelling and control of triple-link pendulum on two wheels system. Triple-link inverted pendulum on two-wheels system

[1]Department of Electrical and Electronics Engineering, Universiti Malaysia Pahang, Pahang, Malaysia
[2]School of Engineering, London South Bank University, London, UK

Corresponding author:
MF Masrom, Department of Electrical and Electronics Engineering, Universiti Malaysia Pahang, Malaysia.
Email: firdausmasrom@gmail.com

has become a significant research topic as it provides more complexity and flexibility in inverted pendulum study. Furthermore, this is a vital research area as there are several current and emerging applications, such as mobile robots, walking robots, and aircraft landing systems, that implement triple-link systems. Moreover, limited work is found on the use of IT2FLC for triple-link inverted pendulum systems, although IT2FLC has been shown as a powerful control technique for non-linear systems.[3]

Over the past decades, FLC has been used in many applications for control with promising success. There are several works done on comparing type-1 fuzzy logic control (T1FLC) and IT2FLC and the results show that IT2FLC is far better than T1FLC.[4] IT2FLC has three-dimensional fuzzy membership function including upper boundary, lower boundary, and footprint of uncertainties which offer additional degree of freedom in order to deal with uncertainties that occur in membership functions. Moreover, IT2FLC has introduced one other element; type reduction before deciding the output from the controller.[5] However, designing a IT2FLC mechanism is complex because it has many parameters that need to be defined before it can work properly and there is no mathematical equation or specific method to determine the best parameter for the controller. Thus, optimisation techniques have been used for acquiring the best parameter values in terms of the shape of the membership function, fuzzy rule, rule base and building the fuzzy sets for the system to work properly.[6] Various optimization algorithms have been used to work with IT2FLC. These include spiral dynamic algorithm (SDA),[7–9] genetic algorithm (GA),[10–16] particle swarm optimization (PSO),[17–21] artificial bee colony (ABC),[22,23] ant colony optimization (ACO),[24] grey wolf optimizer (GWO)[25,26] and hybrid optimization technique.[27,28] The optimization algorithm is used to obtain the best parameters for IT2FLC. For example, hybrid genetic algorithm (HGA) has been used to optimize membership function of IT2FLC, building the fuzzy sets based on membership function, and identify the rule base.[13] The system described in Hamza et al.[19] is based on optimization using artificial bee colony to define a new defuzification method, and applied on the left and right points to obtain the best values inside IT2FLC. The grey wolf optimizer has also been used to tune the parameters of Takagi-Sugeno proportional-integral fuzzy controllers and this has been compared with PSO and GSA in a laboratory servo system.[25]

SDA was introduced by Tamura and Yasuda in 2011.[42] SDA used logarithmic spiral as the model so that the diversification and search strategy can be fulfilled properly as the spiral movement always converges to the centre of the spiral.[7] SDA has successfully been embedded with fuzzy logic control as reported in Ghani et al.,[8] where SDA is used to optimize the input and output scaling factors of a stair climbing wheelchair. The values obtained from SDA have improved the performance of stair climbing in terms of reducing the error of seat and increasing the user's comfort.

PSO was introduced in 1995 by Kennedy and Eberhart.[41] PSO has a simple structure, and thus less computational time is needed.[29] There are several works done on IT2FLC optimization using PSO. The system described in Hassan[18] was the application of PSO to tune the input and output gains for a twin rotor multi input multi output system that used four IT2FLCs to control yaw and pitch axes with their cross coupling of the system. The result in Hassan[18] shows that the performance using PSO based IT2FLC was improved by 17.1%–33%.[17] discussed optimisation of parameters of primary membership function in IT2FLC using PSO and applied to a flexible-joint robot. The simulation results showed that IT2FLC with PSO was far superior in terms of robustness, accuracy, and interpretability.

The main focus of this paper is to design the robust controller to reduce vibration, cater uncertainties and disturbance rejection for a triple-link inverted pendulum on two-wheels system. The model is developed in Simwise 4 D environment for visualization and evaluation purpose. IT2FLC has been selected to control the system. As there are no specific methods or mathematical approach for obtaining the input and output gains of the system, conventional, trial and error method is commonly used. However, this consumes a lot of time for good performance to be achieved. Moreover, trial and error method is an unreliable method as there is no way to ensure that the values from the method are the best values for the system. Therefore, an optimization method using PSO and SDA is proposed in this work and the system performance is assessed in terms of stability and disturbance rejection.

The rest of the paper is organized as follows: The next section describes the modelling of triple-link inverted pendulum on two-wheels system. Then presents the stability control using IT2FLC. The SDA and PSO are described in the subsequent section, respectively. The results of this investigation are presented and discussed in the penultimate section, and the paper is concluded with conclusions.

Modelling of triple-link inverted pendulum on two-wheels system

Triple-link inverted pendulum on two-wheels system has been modelled in four dimensional design software SimWise 4D. This is to retain the complexity of the system and not rely on simplified mathematical modelling.

Moreover, conventional mathematical modelling cannot satisfy human logic and is far from representing the model in the real world. Furthermore, SimWise 4D allows the user to build the model with various types of joint and motor, observe the movement of the model, and test the model with uncertainties and disturbances. SimWise 4D can further be integrated with Matlab/Simulink, allowing controller design and evaluation.

The triple-link inverted pendulum uses the same concept as other inverted pendulum on two-wheeled system. The first link is locked at the centre of the wheel, while the second and third links connected to the first link. Figure 1 shows a diagram of the model where rw is radius of the wheel, while mw, $m1$, $m2$, and $m3$ represent the masses of the wheel, link 1, link 2 and link 3, respectively. The lengths for these three links are represented by $L1$, $L2$, and $L3$. $\theta1$, $\theta2$, and $\theta3$ are the tilt angles of the three links, respectively. The model is built as such so that for all three links to be controlled independently. The model of triple-link inverted pendulum on two-wheels system is built in SimWise 4D because it enables the user to determine the position of motor needed in the model and the input used in the system as shown in Figure 2. The system is modeled in an upright position. The right and left wheels are connected to the base using revolute motors to control the first link since the first link is locked at the base using a rigid joint. The second link is connected to the first link using a revolute motor and it is the same as the third link. The use of revolute motor is to enable the model to become more flexible since it is not in rigid position as the revolute motor can rotate around the y-axis. The parameters for the triple-link inverted pendulum on two-wheels
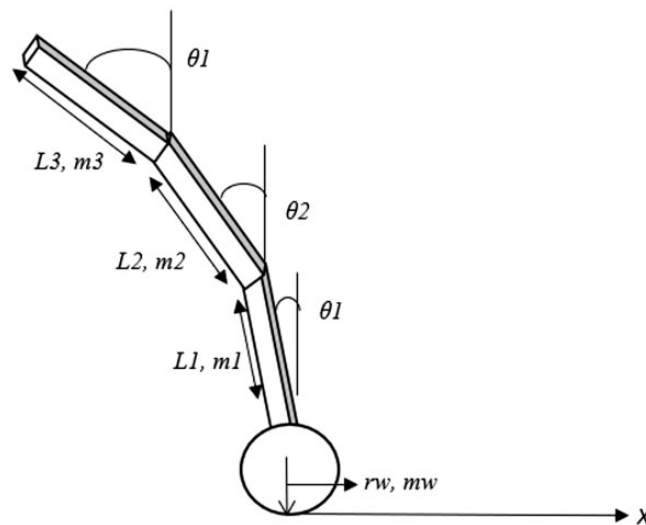

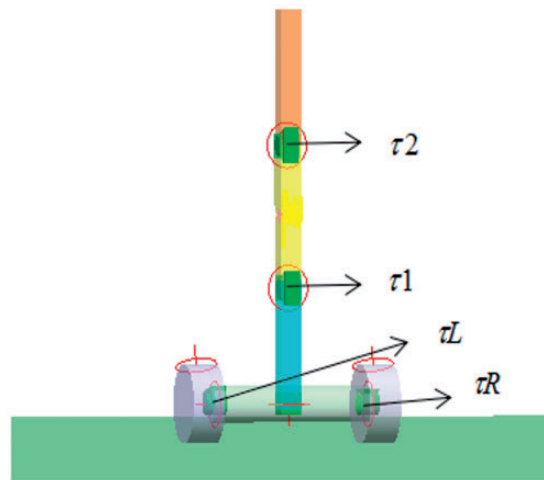**Figure 1.** Schematic diagram of triple-link inverted pendulum on two-wheels system.

Figure 2. Model of triple-link inverted pendulum on two-wheels system in SimWise 4 D.

system are based on previous research[30–32] done on inverted pendulum on two-wheels systems, and these are shown in Table 1.

Interval type-2 fuzzy logic control

Interval type-2 fuzzy logic control (IT2FLC) has been introduced by Zadeh[33] in 1975. IT2FLC consists of five elements, namely fuzzifier, a combination of rule base and database to form knowledge base, inference engine, type-reduction, and defuzzifier as shown in Figure 3. Membership function in IT2FLC is defined by type-2 fuzzy sets. The membership functions used in this work range from –1 to +1 using Gaussian membership function type, which is a better option for a flexible system like the inverted pendulum system. IT2FLC provides a three-dimensional membership function which consists of upper boundary, lower boundary, and footprint of uncertainty in order to give more precise output and eliminate uncertainties in the membership function. Figure 4 shows the membership function graph used in this work.[33,34]

The process in IT2FLC starts with fuzzifier, which is used to fuzzify input crisp values of IT2FLC and converts into type-2 fuzzy sets. The interval type-2 fuzzy sets are defined as[35]

$$\tilde{A} = \int_{x \in X} \int_{uJx \subseteq [0\ 1]} \frac{1}{x, u} = \int_{x \in X} \left[\int_{u \in Jx \subseteq [0\ 1]} \frac{1}{u} \right] /x \qquad (1)$$

Table1. Parameters for triple-link inverted pendulum on two-wheels system.

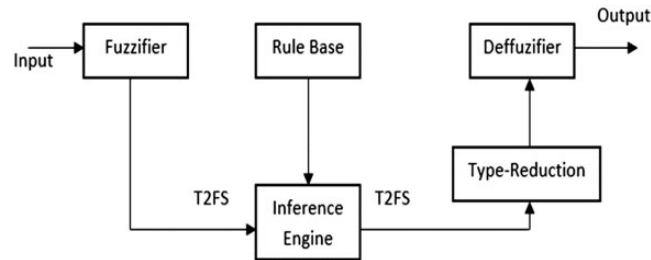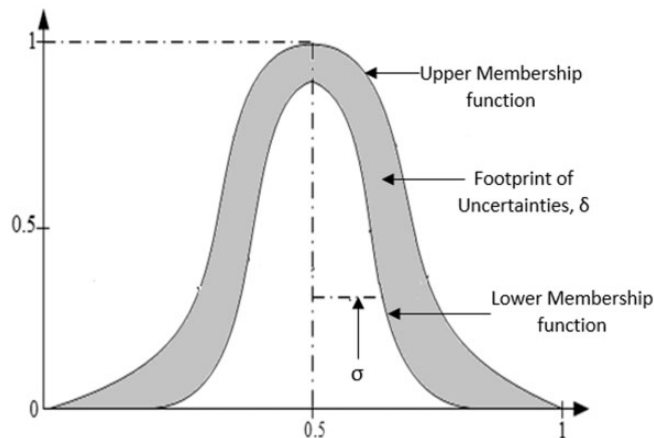| Part	Material	Dimension (m)	Weight (kg)
Wheel	Rubber	Radius = 0.065, Width = 0.06	0.7
Bottom base	Aluminium	Radius = 0.03, Length = 0.3	1.5
Link 1	Aluminium	Width = 0.04, Length = 0.04, Height = 0.22	3
Link 2	Aluminium	Width = 0.04, Length = 0.04, Height = 0.22	3
Link 3	Aluminium	Width = 0.04, Length = 0.04, Height = 0.22	3

Figure 3. Block diagram of IT2FLC.

Figure 4. IT2FLC Gaussian membership function.

$$Jx = \left\{ (x, u) : u \in \left[\underline{\mu}_{\tilde{A}}(x), \overline{\mu}_{\tilde{A}}(x) \right] \right\} \tag{2}$$

where x is a primary variable, while u is a secondary variable and Jx is a domain for each variable called the primary membership of x. The footprint of uncertainties (FOU) is the union of primary membership for fuzzy sets. $\overline{\mu}_{\tilde{A}}(x)$ is the upper membership function (UMF), whereas $\underline{\mu}_{\tilde{A}}(x)$ is the lower membership function (LMF) associated with upper and lower bound of footprint of uncertainties as given by[35]

$$\underline{\mu}_{\tilde{A}}(x) = \overline{FOU(A)} \ \forall x \in X \tag{3}$$

$$\overline{\mu}_{\tilde{A}}(x) = \underline{FOU(A)} \forall x \in X \tag{4}$$

$$FOU(\tilde{A}) = \underset{\forall x \in X}{U} Jx = \left\{ (x, u) : u \in Jx \subseteq [0 \ 1] \right\} \tag{5}$$

The rule base is determined and defined so as to achieve the performance objectives of the work. Five linguistic variables are defined as negative big (NB), negative small (NS), zero (Z), positive small (PS), and positive big (PB) for IT2FLC inputs and outputs resulting in 25 rules as shown in Table 2. The fuzzy rules are formed as:

If x is A and y is B then z is C

where A and B are the two inputs of the IT2FLC and C is the output which will be used for stabilizing control.

The five membership functions used have their specific properties for each input. Firstly, they are centred at –1, –0.5, 0, 05, and 1. Second, they have the specific uncertain means, δ and standard deviation, σ in order to determine the size of membership function. The standard value for uncertain mean is 0.125, while for standard deviation is 0.418. These values are optimized in this work to find the optimal shape of the membership function for the system to work efficiently.

Before producing the IT2FLC outputs, type reduction method is performed to get the crisp output values. Nie-Tan type reduction is chosen in this work because it has been proven to be better compared to normal Karnik Mendel type reduction.[36] This is because it can produce outputs with better precision and faster due to the use of average value in membership function as[36]

$$Y = \frac{\sum_{n=1}^{N} Y^n \left(\underline{f^n} + \overline{f^n} \right)}{\sum_{n=1}^{N} \left(\underline{f^n} + \overline{f^n} \right)} \tag{6}$$

The stabilizing control is designed in Simulink/Matlab as shown in Figure 5. Figure 5 is the Simulink block diagram showing the usage of input output gains and switch to produce torque for the system. This system requires four loops to produce four values of torque in order to stabilize all three links. The error and change of error are obtained and used as inputs of the IT2FLC and the output produced is used to control the system.

An optimization algorithm is proposed to find the optimal values of input output value gains and IT2FLC parameters which are σ and δ for stabilizing triple links inverted pendulum on two-wheeled system. Conventionally, heuristic tuning of the control parameters was used but such heuristic method does not guarantee

Table 2. Rule base for IT2FLC.

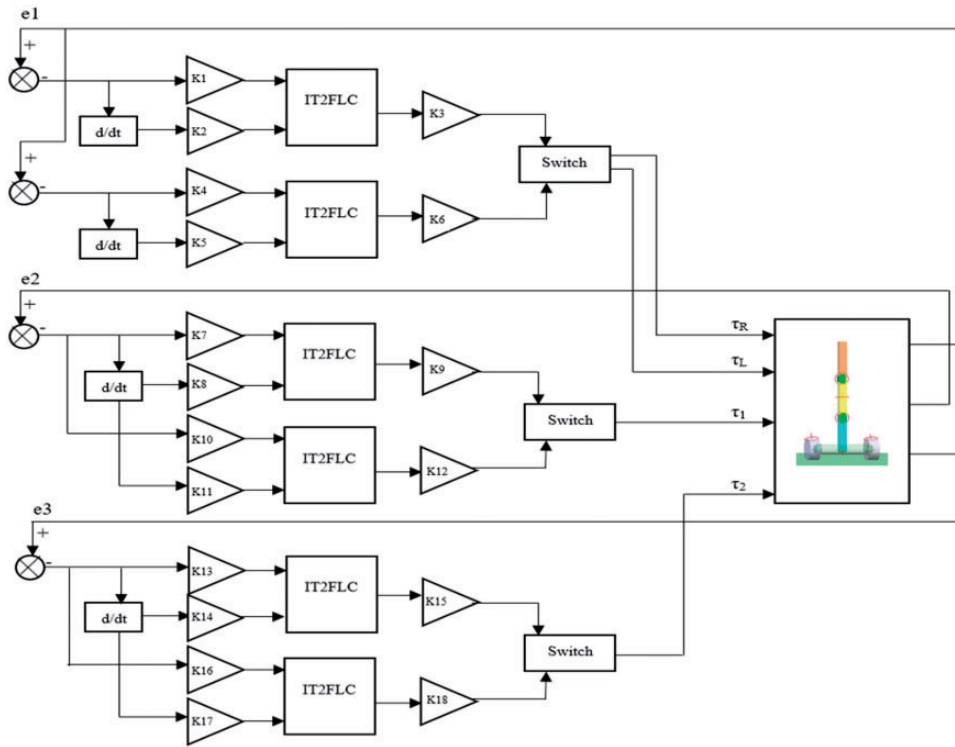| d\ e	NB	NS	Z	PS	PB
NB	PB	PB	PB	PS	Z
NS	PB	PB	PS	Z	NS
Z	PB	PS	Z	NS	NB
PS	PS	Z	NS	NB	NB
PB	Z	NS	NB	NB	NB

Figure 5. Simulink block diagram block diagram.

that it will produce the best result. A global optimisation mechanism such as spiral dynamic algorithm (SDA) and particle swarm optimization (PSO) is necessary to improve the system performance. Due to its significant advantages over other searching methods, an optimization approach is used to optimise the control input and output gains along with IT2FLC control parameters

In this study, the objective of fitness function of the optimization is to minimize the error of angular position of Link 1, angular position of Link 2 and angular position of Link 3, while the system stabilizes these three links to ensure the stability of triple links inverted pendulum on two-wheeled system at the upright position. The root mean square error (RMSE) was chosen as the fitness function in this work,

$$RMSE = \sqrt{\frac{1}{N}\sum_{i=1}^{N}(e^2)} \tag{3.39}$$

The fitness function of the system in this research is a summation of RMSE functions of the angular position by taking the sum of weightage of all three links, where the weight vector of this system is $[w_1\ w_2\ w_3] = [0.4\ 0.3\ 03]$. Noted that w_1 represents weight at Link 1, w_2 represents weight at Link 2 and w_3 represents weight at Link 3 respectively. Weight at Link 1 was chosen to be the highest ratio because Link 1 is more crucial in stabilizing the whole system compared to Link2 and Link 3. The fitness function is, *Fitness Function* $= w_1 MSE_1 + w_2 MSE_2 + w_3 MSE_3$, where MSE_1 represents the error of angular position of Link 1, MSE_2 is for the error of angular position of Link 2 and MSE_3 is for the error of angular position of Link 3, respectively.

Spiral dynamic algorithm

SDA is known as a metaheuristic optimization inspired by natural spiral patterns such as tornado, hurricanes, and galaxy introduced by Tamura and Yasuda,[42] whose initial work was focused on two-dimensional problems and later extended to nth dimensional problems. The most essential aspect in SDA is the balanced combination of exploration and exploitation strategies. In SDA, all the search agents are designed to move from the outermost area to the centre of the spiral and move toward the centre of the spiral as the number of iterations increase.
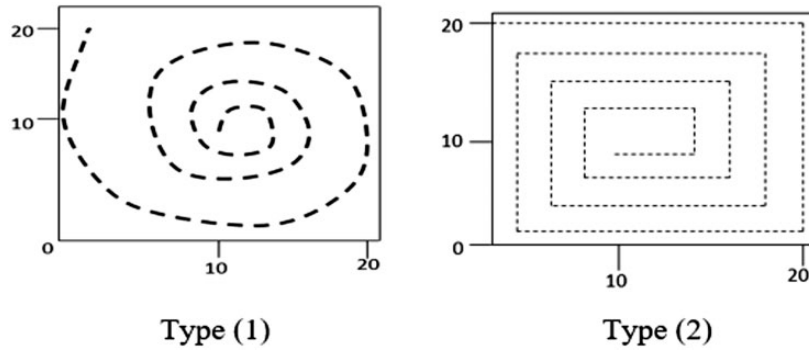
Figure 6. Types of spiral shape in SDA. Type (1) $\theta = \pi/4$; Type (2) $\theta = \pi/2$.

This is known as the intensification phase where it happens in the inner area of the spiral toward the centre. The mathematical model for SDA is defined as[8]

$$\chi_i(k+1) = S_n(r,\theta)\chi_i(k) - [S_n(r,\theta) - I_n]\ \chi*, \quad i = 1,2,3,\ldots\ldots,m \tag{7}$$

where θ is the angle of rotation which varies from 0 to 2π, I_n is a matrix, $\chi*$ is the center of the spiral, k is the number of iterations, r is the radius of the spiral, which ranges from 0 to 1, i is the number of points, and m is the maximum point.[7]

Figure 6 shows a couple of examples of spiral shapes in SDA and movements of the search agents from the outermost area towards the centre of the spiral. Figure 7 shows a flowchart of SDA implementation.[8]

In this work, radius, $r = 0.95$ and $\theta = \pi/4$ are used for the spiral dynamic trajectory. The number of search agents is 50, while the number of iteration used in this work is 40. The objective of this optimization is to minimize the angular position error and manage external disturbance. All the 18 inputs and output gains along with δ and σ are used in determining the size of membership function in the IT2FLC.

Particle swarm optimization

PSO is one of the metaheuristic techniques inspired by the behaviour of group of animals for instance flock of birds and the schools of fish. PSO was introduced by Eberhart and Kennedy in 1995[37] and has been applied in various applications such as signal processing, optimal design, and data mining. PSO uses a population-based method where the state of the algorithm is represented by population and modified repeatedly until the objective is achieved.[37–40]

In PSO, the particle will move based on the current optimum particles. All particles will keep their tracks in the area in which the best solution or *pbest* is achieved. The best value among all the particles is the global best, or *gbest*, and is obtained by considering finesses of all the particles in the population. The concept of PSO is to update the velocities and positions of each particle towards its *pbest* according to equations (8) and (9)

$$V_i(k+1) = wV_i(k) + c1 * rand * (P_i(k) - X_i(k)) + c2 * rand * (g(k) - X_i(k)) \tag{8}$$

$$x_i(t+1) = x_i(t) + v_i(t+1) \tag{9}$$

where V_i is the velocity of the particle, X_i is the particle position, w is the inertial weight, k is the iteration, *rand* is the random value between 0 to 1, $c1$ is the cognitive acceleration coefficient and $c2$ is the social acceleration coefficient. The values for $c1$ and $c2$ are chosen as 2.[37] The inertia weight is decreased from 0.9 to 0.4 during the optimization. Figure 8 shows the flowchart of PSO implementation.[37]

Similar to SDA, PSO is used to find optimal values for the 18 input and output gains of the system and the σ and δ values for membership function of IT2FLC. These 20 parameters need to be optimized to enhance the performance of IT2FLC control in triple links inverted pendulum on two-wheeled system.

Results

The results of this study are presented and discussed in detail with reference to the objective of this study, which is to assess the effectiveness of implementing IT2FLC based on PSO on triple-link inverted pendulum on two-wheels
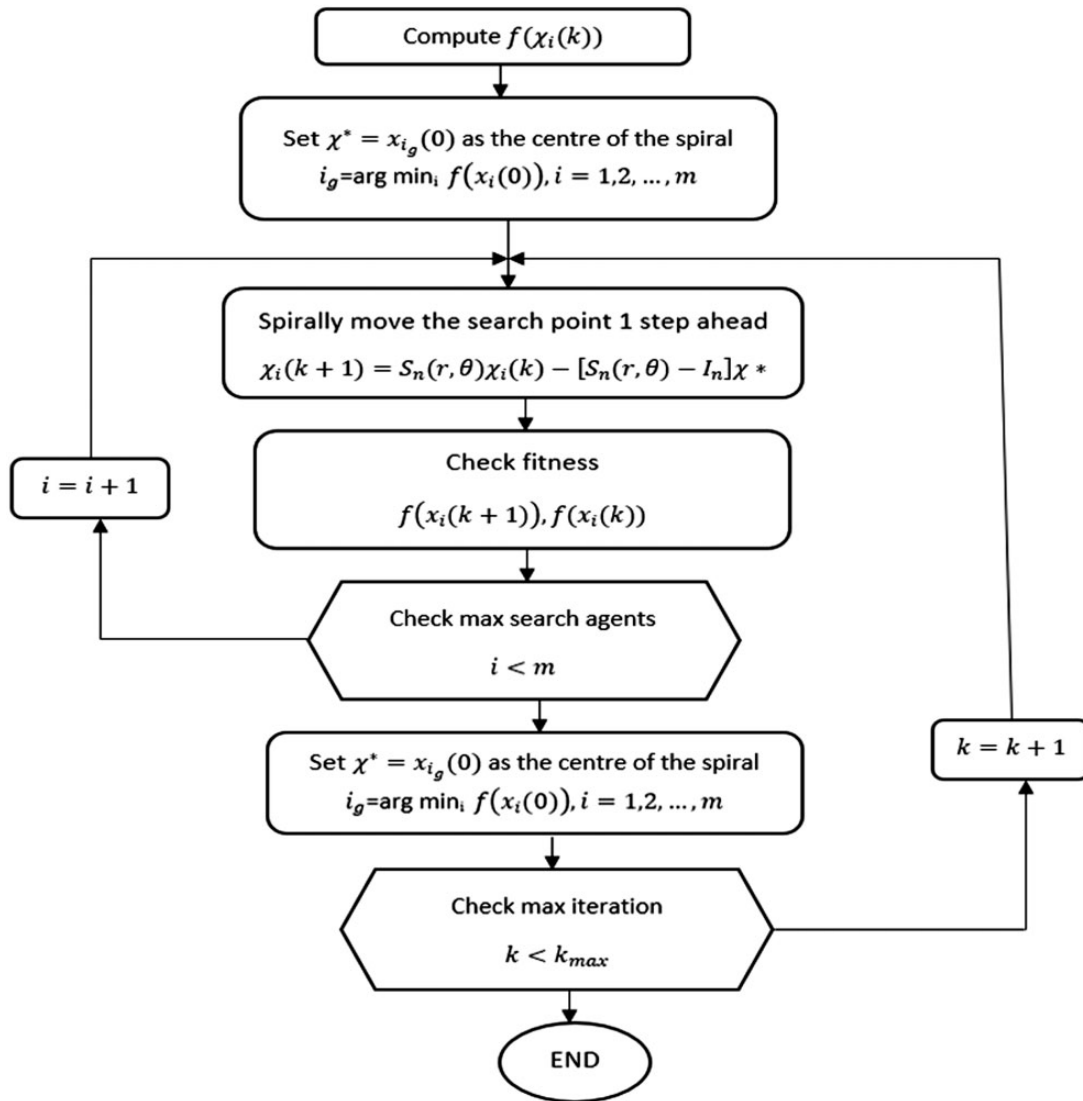
Figure 7. SDA flowchart.

system. The results are obtained in simulated exercises using an integrated Matlab/Simulink and SimWise 4D environment. Two optimization algorithms, namely PSO and SDA are used in the design of the controller and a comparative assessment of the system performance is carried out.

Fitness function for optimization algorithm

Figures 9 and 10 show the convergence graphs of SDA and PSO as function of number of iterations, respectively. As noted, PSO has performed significantly better than SDA, where the PSO and SDA began their exploration phases with fitness function values of 0.01281 and 0.01769, respectively. The exploitation phases of the algorithms began when the fitness function values decreased to 0.0077 for PSO and 0.01753 for SDA. The best fitness function value for PSO was 0.00578, while for SDA it was 0.01752. This shows that PSO has a better convergence compared to SDA. A trial and error approach was also used for obtaining the system input and output gains and the σ and δ values for membership function of IT2FLC. These are shown with optimised values in Table 3.

Stability control

The main objective for this research is to achieve stable performance of the triple-link inverted pendulum on two-wheels system. The objective is achieved by using the input output gain values obtained in the control system. The
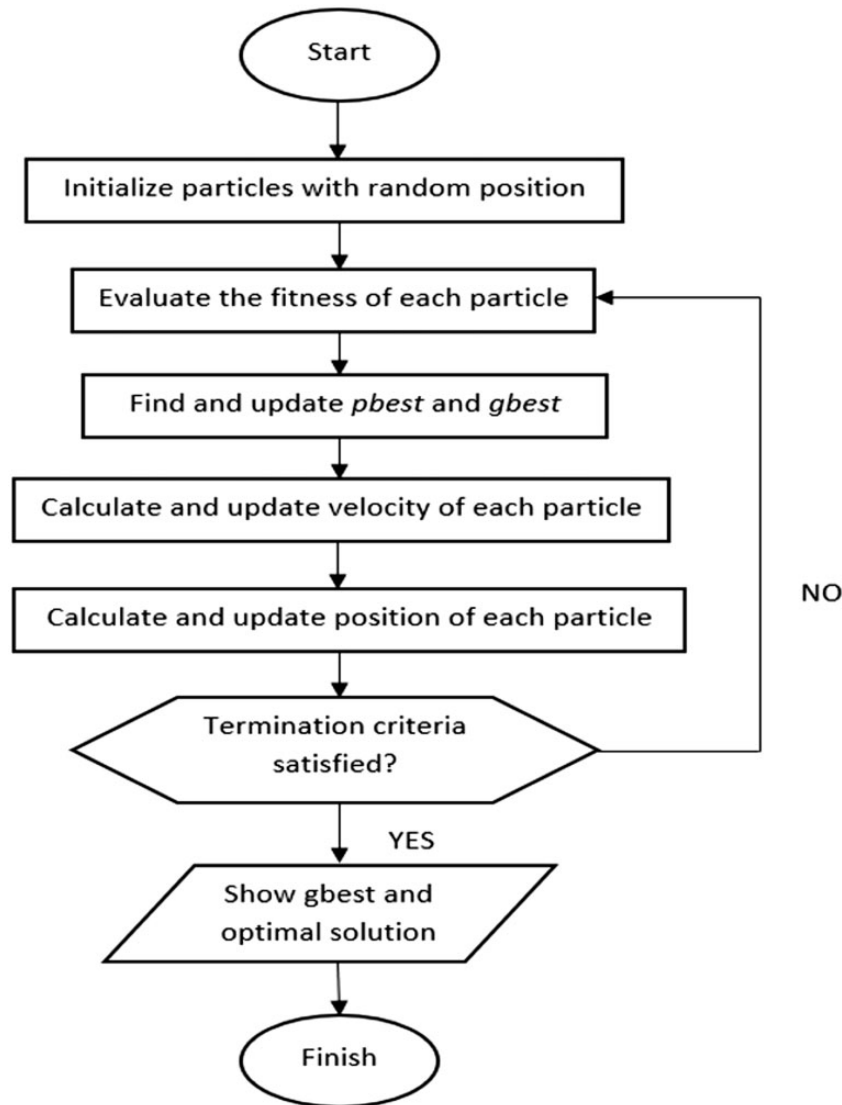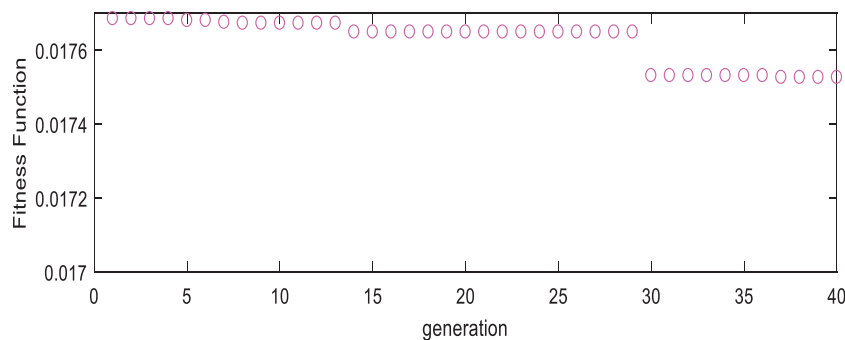
Figure 8. Flowchart of PSO.

Figure 9. Fitness function graph for SDA optimization.

values will determine the control torque for actuating the motors. The system performances using the control parameters obtained by the trial and error, SDA and PSO approaches are shown in Figures 11 to 13 and Table 4.

The performances shown in Figures 11 to 13 and Table 4 are assessed in terms of peak overshoot, peak under-shoot, and angular position for all the three links. As noted the PSO-based system has performed well for both Link
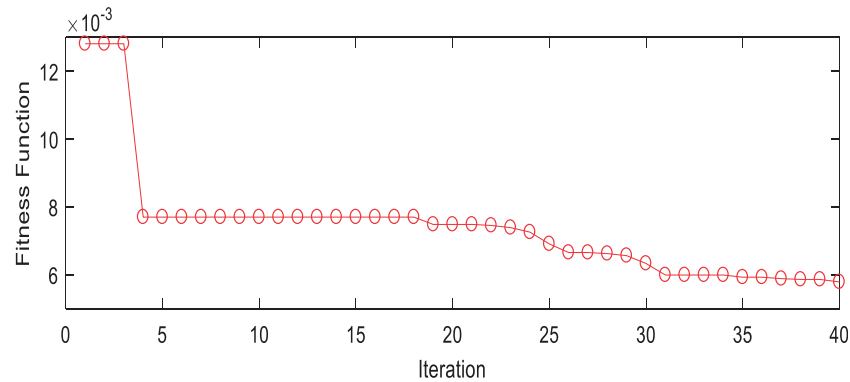
Figure 10. Fitness function graph for PSO optimization.

Table 3. Input output gains.

Gain	Trial and error	SDA	PSO
K1	0.117	0.1129	0.1125
K2	0.0034	0.0035	0.0037
K3	90	92.8359	88.2941
K4	0.4	0.4177	0.4159
K5	0.005	0.0046	0.0045
K6	75	76.9662	77.1807
K7	0.043	0.0413	0.0439
K8	0.0064	0.0069	0.006
K9	100	103.8641	99.0602
K10	0.2	0.2015	0.2216
K11	0.01	0.0118	0.0142
K12	80	84.7679	84.8402
K13	0.7	0.6625	0.7483
K14	0.004	0.0043	0.0044
K15	120	123.2705	123.657
K16	0.085	0.0878	0.088
K17	0.004	0.0037	0.0041
K18	85	84.2864	84.1887
Δ	0.125	0.1201	0.1213
Σ	0.418	0.4163	0.4195

1 and Link 2 in angular position as the errors are relatively smaller than those achieved with SDA and trial and error methods. As for link 3, the SDA-based system performed slightly better than PSO, where the angular position error with SDA was –0.4279° compared to PSO-based error of –0.4322°. Figures 14 to 16 show the control effort (torque) generated for stabilizing the three links. As noted the links settled in 5 s but fluctuated in the early stages, as expected.

In comparison to previous research done on triple-link inverted pendulum system, the current result is better by 66% and 53.6% when compared to triple-link inverted pendulum on cart system in Sharma and Sahu[1] in terms of peak overshoot. This is a very significant improvement because even though the pendulum on cart system has been shown to have a better stability compared to that on two-wheels system, the current system has outperformed the inverted pendulum on cart system. Moreover, the system in Sharma and Sahu[1] has used conventional mathematical modelling which cannot satisfy a real-world system compared with the current system, which uses CAD-based software SimWise 4D that is able to retain the complexity and flexibility of the system.

Comparing the results achieved a two-wheeled system described in paper,[30] one notices that the system in the two-wheeled system needed approximately 10 s to achieve stability, while the current system only needs 5 s to achieve the same goal even though this system is more complex with three links, while the two-wheeled system in Ahmad et al.[30] is a double-link system. Moreover, the angular position for the system in Ahmad et al.[30] was maintained at 0.7° for the first link and 0.3° for the second link. The current work shows improvements of 33.3%
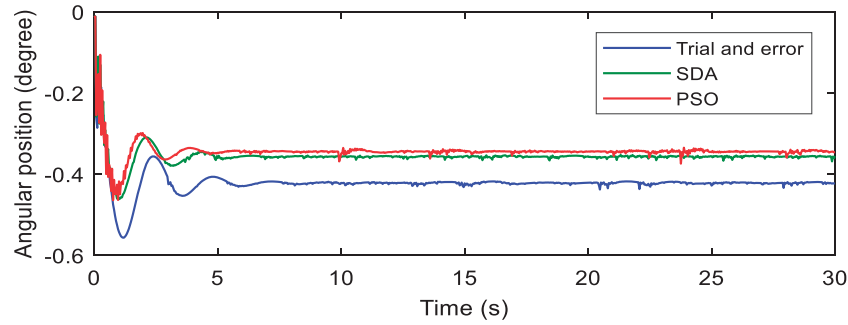
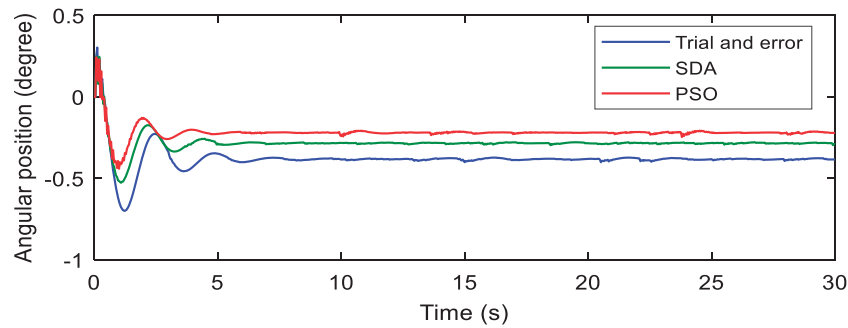**Figure 11.** Angular position of Link 1.
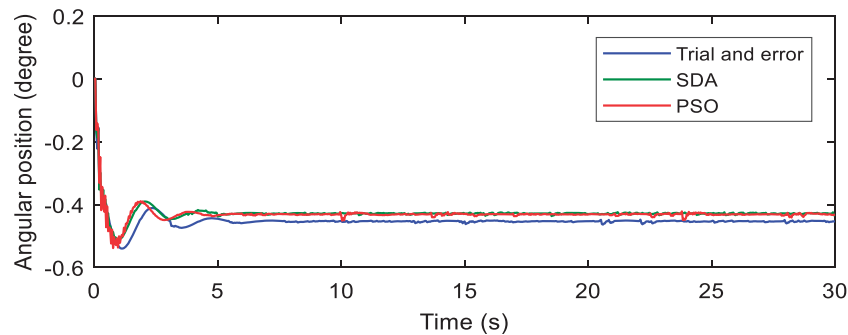

Figure 12. Angular position of Link 2.

Figure 13. Angular position of Link 3.

Table 4. Position errors using the trial and error, SDA, and PSO approaches.

	Peak Overshoot (degrees)			Peak Undershoot (degrees)			Angular position (degrees)		
	Trial and error	SDA	PSO	Trial and error	SDA	PSO	Trial and error	SDA	PSO
Link 1	−0.3561	−0.309	−0.2992	−0.5532	−0.4582	−0.4645	−0.4212	−0.3752	−0.3433
Link 2	−0.2283	−0.1752	−0.1298	−0.6959	−0.5176	−0.4376	−0.3827	−0.2833	−0.2207
Link 3	−0.4114	−0.3904	−0.3894	−0.5398	−0.5077	−0.5386	−0.4538	−0.4279	−0.4322

for the first link and 51.4% for the second link in terms position error. Table 5 shows the complete table of performance comparison with previous work in stability focuses on lower vibrations for the system.

Disturbance rejection

In order to test the robustness of the controller, disturbances were applied to the system and the system response assessed. The disturbances considered were in the form of pulses applied at the back of Link 3.
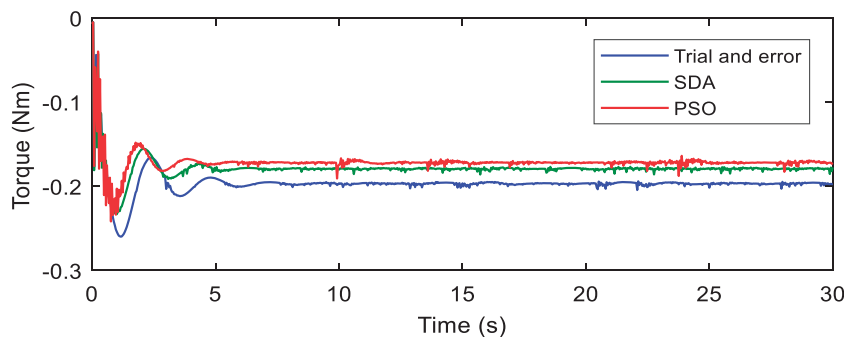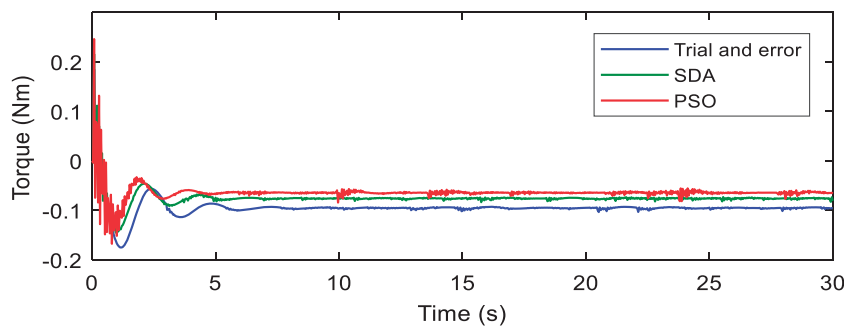
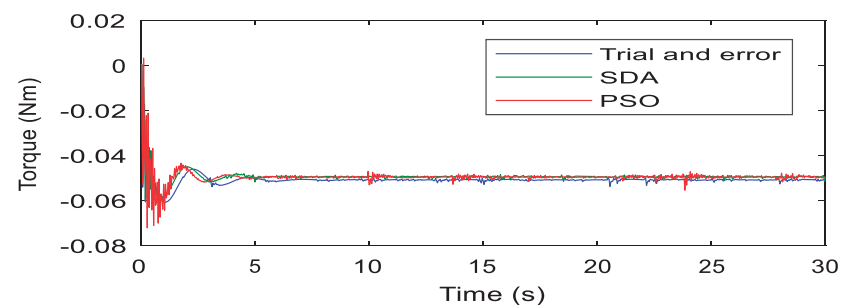**Figure 14.** Torque value at Link 1.

Figure 15. Torque value at Link 2.

Figure 16. Torque value at Link 3.

Table 5. Comparison with previous work based on stability performance.

| Aspect \ Paper	Firdaus, 2019	Gupta et al.[43]	Sharma and Sahu[1]	Jun-Wei et al.[44]	Ahmad et al.[30]
System	Triple links inverted pendulum on two-wheeled system	Triple links inverted pendulum on cart system	Triple links inverted pendulum on cart system	Triple links inverted pendulum on cart system	Double links inverted pendulum on two-wheeled system
Controller	IT2FLC-based PSO	LQR	LQR	LQR	T1FLC
Settling time (second)	5	4	3.5	5	8
Angular position (degree)	−0.3, −0.2, −0.4	0.05, 0, 0	0, 0, 0	0, 0, 0	0.7, 0.3
Peak overshoot (degree)	−0.3, 0.13, −0.39	0.5, 0.02, 0.013	0.9, 0.3, 0.2	0.7, 0.7, 0.9	0.8, 3.0
Peak undershoot (degree)	−0.46, −0.44, −0.54	−0.5, −0.03, −0.012	−0.58, −0.36, −0.22	−1.4, −1.6, −2.6	0, 0
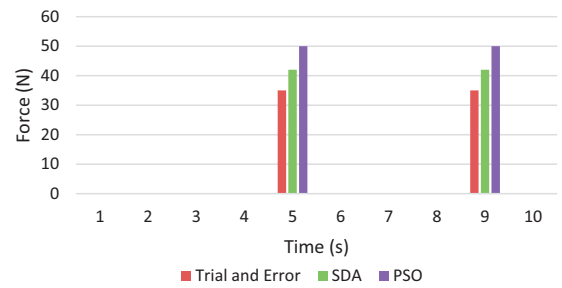
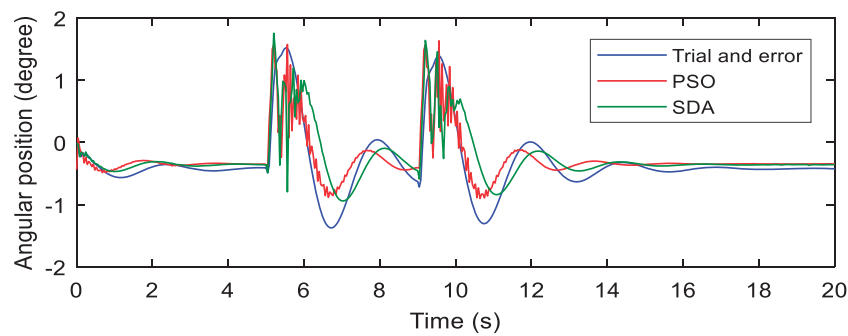**Figure 17.** Maximum disturbance at Link 3.

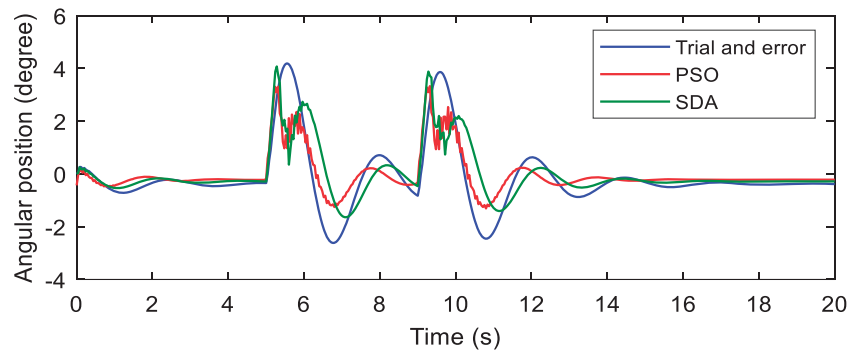**Figure 18.** Angular position of Link 1.

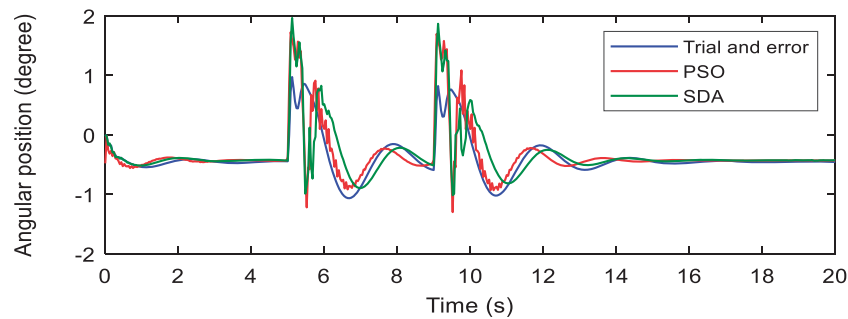**Figure 19.** Angular position of Link 2.

Figure 20. Angular position of Link 3.

Table 6. Performance comparison on disturbance rejection with previous work.

Aspect \ Paper	Firdaus, 2019	Muhammad et al.[45]	Almeshal et al.[46]
System	Triple links inverted pendulum on two-wheeled system	Single link inverted pendulum on two-wheeled system	Double links inverted pendulum on two-wheeled system
Controller	IT2FLC-based PSO	State feedback tracking controller	PD controllers
Disturbance value (N)	50	30	20
Settling time after disturbance (second)	4	8	6
Peak angle (degree)	3.8	1.2	0.13

Based on the graph shown in Figure 17, the maximum disturbance rejected by PSO was 50 N, while by SDA it was 42 N, and by trial and error method was 35 N. This shows that PSO was the best optimization for this triple-link inverted pendulum on two-wheels system. Figures 18 to 20 show the system responses when the disturbance was applied at 5 and 9 s influencing the system to move forward and needed about 3 s to achieve stability back after it had been disturbed. It is noted that the trial and effort-based system was affected the most due to application of the disturbance. It is further noted that Link 2 was the most affected as it moved up to 4° for SDA and trial and error method but with the PSO, the system moved to 3.8° only.

Table 6 shows the comparison done on previous work in two-wheeled mobile robot since there are no work found on disturbance rejection for triple links inverted pendulum system. From this table, the proposed controller managed to withstand the highest value of force applied to it compared to other with 50 N. Moreover, this system has the lowest settling time with 4 s, while system proposed by Mustafa need 8 s and Almeshal's system need 6 s to settle.

Conclusion

In this paper, a control design approach by adoption of optimization techniques based on SDA and PSO has been proposed in the paper for tuning of control parameters of IT2FLC for triple-link inverted pendulum on two-wheels system. The aim of the optimization is to enhance the efficiency of the system in terms of stability and disturbance rejection. A proposed controller has been successfully implemented and tested in this paper, and the performance of the system was observed within simulated exercise through SimWise 4 D visualization software integrated with Simulink in Matlab.

The results have shown superior performance of the PSO-based system over SDA-based system by 9.3% and 28.4% in angular position errors of Link 1 and Link 2, respectively. Furthermore, peak values of SDA were higher than PSO which means that PSO has lower noise than SDA and more stable; this system has been proven to have lower peak overshoot and settling time compared to previous work.

It has been proved that the proposed controller in this paper managed to withstand higher disturbance compared to previous work by 66.7%. Moreover, the settling time after disturbance that was applied has significantly improved with only 4 s compared to 8 and 6 s from previous research. In the future work, the system will be test on linear motion in smooth surface, rough surface and inclined surface to further test the robustness of the controller. Besides that, this controller could be implemented in real-hardware applications.

Declaration of conflicting interests

Funding

ORCID iD

MF Masrom https://orcid.org/0000-0003-3041-3044

References

1. Sharma K and Sahu V. Modeling and stabilization of cart triple link inverted pendulum using LQR controller incorporating degree of stability. *Int Res J Adv Eng Sci* 2016; 1: 148–152.
2. Wei GJ, Qiang CG, Jian JZ, et al. Adaptive neural-fuzzy control of triple inverted pendulum. *Control Theor Appl* 2010; 27: 3–7.
3. Naik KA. Performance comparison of type-1 and type-2 fuzzy logic systems. In: *4th IEEE international conference on signal processing, computing and control*, (ISPCC 2017), Solan, India. 21-23 September 2017, pp.72–76.
4. Castillo O, Amador-Angulo L, Castro JR, et al. A comparative study of type-1 fuzzy logic systems, interval type-2 fuzzy logic system and generalized type-2 fuzzy logic system in control problems. Information Sciences—Informatics and Computer Science, Intelligent Systems, Applications: An International Journal, 2016; 354: 257–274.
5. Chotikunnan P and Panomruttanarug B. The application of fuzzy logic control to balance a wheelchair. *Control Eng Appl Inform* 2016; 18: 41–51.
6. Castillo O and Melin P. A review on the design and optimization of interval type-2 fuzzy controllers. *Appl Soft Comput J* 2012; 12: 1267–1278. no.
7. Hashim MR and Tokhi MO. Greedy spiral dynamic algorithm with application to controller design. *IEEE Conf Syst Proc Control* 2016; 29–32.
8. Ghani NMA, Nasir ANK and Tokhi MO. Optimization of fuzzy logic scaling parameters with spiral dynamic algorithm in controlling a stair climbing wheelchair : ascending task. In: *19th international conference on methods and models in automation and robotics*, Międzyzdroje, Poland, 2-5 September, 2014, pp. 776–781.
9. Nasir ANK, Tokhi MO and Sayidmarie O. A novel adaptive spiral dynamic algorithm for global optimization. In: *2012 IEEE 11th International Conference on Cybernetic Intelligent Systems (CIS)*, Limerick, 23-24 August 2012, pp. 99–104. Piscataway, NJ: IEEE.
10. Lu X and Liu M. Optimal design and tuning of pid-type interval type-2 fuzzy logic controllers for delta parallel robots. *Int J Adv Robot Syst* 2016; 13: 1–12.
11. Hinojosa EC and Camargo HA. Multi-objective evolutionary algorithm for tuning the Type-2 inference engine on classification task. *Soft Comput* 2018; 22: 5021–5031.
12. Yeasmin S, Paul AK and Shill PC. Optimization of interval type-2 fuzzy logic controllers with rule base size reduction using genetic algorithms. In: *3rd international conference on electrical engineering and information communication technology (ICEEICT)*, Dhaka, Bangladesh, 22-24 September 2016.
13. Martínez R, Castillo O and Aguilar LT. Optimization of interval type-2 fuzzy logic controllers for a perturbed autonomous wheeled mobile robot using genetic algorithms. *Inform Sci* 2009; 179: 2158–2174.
14. Shill PC, Amin F, Akhand MAH and Murase K. Optimization of interval type-2 fuzzy logic controller using quantum genetic algorithms. *2012 IEEE International Conference on Fuzzy Systems*, Brisbane, Australia, 2012, pp. 1–8.
15. Castillo O, Melin P, Alanis A, et al. Optimization of interval type-2 fuzzy logic controllers using evolutionary algorithms. *Soft Comput* 2011; 15: 1145–1160.
16. Kulkarni AG, Qureshi MF and Jha M. Genetically tuned interval type-2 fuzzy logic for fault diagnosis of induction motor. *Int J Innov Res Sci Eng Technol* 2007; 3: 14890–14899.
17. Zirkohi MM. Type-2 fuzzy control for a flexible-joint robot using voltage control strategy. *Int J Autom Comput* 2013; 10: 242–255.
18. Hassan MY. Intelligent tracking control using PSO-based interval type-2 fuzzy logic for a MIMO maneuvering system. *Al-Qadisiyah J Eng Sci* 2018; 11: 22–39.
19. Hamza MF, Yap HJ and Choudhury IA. Genetic algorithm and particle swarm optimization based cascade interval type 2 fuzzy PD controller for rotary inverted pendulum system. *Math Prob Eng* 2015; 2015: 1–15.
20. Hein D, Udluft S and Runkler TA. Generating interpretable fuzzy controllers using particle swarm optimization and genetic programming. *GECCO '18 Proceedings of the Genetic and Evolutionary Computation Conference Companion* Kyoto, Japan, 15–19 July 2018. pp. 1268–1275.
21. Choeychuen K. Fuzzy membership function optimization for smart LED lamp using particle swarm optimization. In: *International workshop on advanced image technology (IWAIT)*, Chiang Mai, Thailand, 7–9 January 2018.
22. Castillo LAO and Amador-Angulo L. A new fuzzy bee colony optimization with dynamic adaptation of parameters using interval type-2 fuzzy logic for tuning fuzzy controllers. *Soft Comput* 2018; 22: 571–594.
23. Kumar A. Artificial bee colony based design of the interval type-2 fuzzy PID controller for robot manipulator. In: *Proceedings of the region 10 conference (TENCON)*, Malaysia, 5-8 November 2018, pp.602–607. Piscataway, NJ: IEEE.
24. Olivas F, Valdez F, Castillo O, et al. Ant colony optimization with dynamic parameter adaptation based on interval type-2 fuzzy logic systems. *Appl Soft Comput* 2107; 53: 74–87.

25. Precup R and David R. An easily understandable grey wolf optimizer and its application to fuzzy controller tuning. *Algorithms* 2017; 10: 1–15.
26. Barraza J, Rodríguez L, Castillo O, et al. A new hybridization approach between the fireworks algorithm and grey wolf optimizer algorithm. *J Optim* 2018; 2018: 1–18.
27. Kumar A and Kumar V. Performance analysis of optimal hybrid novel interval type-2 fractional order fuzzy logic controllers for fractional order systems. *Exp Syst Appl* 2018; 93: 435–455.
28. Abdalla TY and Allawi ZT. An optimized interval type-2 fuzzy logic control scheme based on an optimized interval type-2 fuzzy logic control scheme based on optimal defuzzification. *Int J Comput Appl* 2014; 95: 26–31.
29. Vu VT. A comparison of particle swarm optimization and differential evolution. *Int J Soft Comput* 2012; 3: 13–30.
30. Ahmad S, Aminnuddin M and Shukor MASM. Modular hybrid control for double-link two-wheeled mobile robot. In: *4th International Conference on Computer and Communication Engineering (ICCCE 2012)*, Kuala Lumpur, Malaysia, 3–5 July 2012.
31. Goher KM and Tokhi MO. A new configuration of two-wheeled inverted pendulum: a Lagrangian-based mathematical approach. *Cyber J* , December Edition 2010: pp.1–5.
32. Urakubo T, Tsuchiya K and Tsujita K. Motion control of a two-wheeled mobile robot. *Adv Robot* 2012; 15: 711–728.
33. Li J and Yang L. Interval Type-2 TSK + fuzzy inference system. In: *IEEE international conference on fuzzy systems*, Rio de Janeiro, Brazil, 8–13 July 2018.
34. Cosenza B and Galluzzo M. Experimental comparison of type-1 and type-2 fuzzy logic controllers for the control of level and temperature in a vessel. *Comput Aid Chem Eng* 2011; 29: 803–807.
35. Ri M, Huang J, Ri S, et al. Design of interval type-2 fuzzy logic controller for mobile wheeled inverted pendulum. In: *12th world congress on intelligent control and automation (WCICA)*. Guilin, China, 12–15 June 2016, pp.535–540.
36. Kumar D and Ghosh R. Novel interval type-2 fuzzy logic controller for improving risk assessment model of cyber security. *J Inform Security Appl* 2018; 40: 173–182.
37. Aote SS, Raghuwanshi MM and Malik L. A brief review on particle swarm optimization : limitations & future directions. *Int J Comput Sci Eng* 2013; 2: 196–200.
38. Sendren HH and Chiang SXC. Optimal fuzzy controller design using an evolutionary strategy-based particle swarm optimization for redundant wheeled robots. *Int J Fuzzy Syst* 2015; 17: 390–398.
39. Alam MS and Tokhi MO. Dynamic modelling of a single-link flexible manipulator system : a particle swarm optimisation approach. *J Low Frequency Noise Vib Active Control* 2007; 26: 57–72.
40. Julai S and Tokhi MO. Vibration suppression of flexible plate structures using swarm and genetic optimization techniques. *J Low Frequency Noise Vib Active Control* 2010; 29: 293–318.
41. Kennedy J and Eberhart R. Particle swarm optimisation. In: *Proceedings of IEEE international conference on neural networks*, Perth, Western Australia, 27 November – 1 December 1995, pp.1942–1948. Piscataway, USA: IEEE Press.
42. Tamural K and Yasuda K. Primary study of spiral dynamics inspired optimisation. *IEEJ Trans Elec Electron Eng* 2011; 6: 98–100.
43. Gupta MK, Bansal K and Singh AK. Stabilization of triple link inverted pendulum system based on LQR control technique. In: *International conference on recent advances and innovations in engineering (ICRAIE)*, Jaipur, 9-11 may 2014, pp.1–5.
44. Jun-Wei G, Guo-Qiang C, Zhi-Jian J, et al. Adaptive neural-fuzzy control of triple inverted pendulum. *Control Theory Appl* 2010; 27: 278–282.
45. Muhammad M, Buyamin S, Ahmad MN, et al. Multiple operating points model-based control of a two-wheeled inverted pendulum mobile robot. *Int J Mech Mech Eng* 2013; 13: 1–9.
46. Almeshal AM, Goher KM and Tokhi MO. Dynamic modelling and stabilization of a new configuration of two-wheeled machines. *Robot Autonomous Syst* 2013; 61: 443–472.